

## CHAPTER 7

### Lithofacies Classification

Rock physics and AVO are dependent on mineralogy (i.e. lithology) and fluid properties. Elastic properties which were obtained from rock physics and AVO analysis were used to describe each lithofacies. Lithofacies can therefore be classified using elastic attributes, such as acoustic impedance, shear impedance and  $V_p/V_s$  (or Poisson's ratio), density, etc., derived from well log data. The objective of the lithocube analysis is to produce a spatial lithology distribution based on lithoclasses, which are defined by petrophysical properties and seismic responses of elastic inversion products.

Facies and Fluids Probability (FFP) is a software module in the Jason software suite that was used for lithofacies classification in this study. FFP is to create lithology probability volumes using deterministic inversion results. The method incorporates estimated uncertainties resulting for example from property overlap of the lithologies, limitations in seismic resolution and the impact of seismic noise. The main assumptions of FFP include:

- Analysis of geologic zones can be completely represented by a set of discrete lithotypes defined by differences in fluid and/or facies.
- Well log data and elastic parameters logs in which a lithology log has also been created to identify each sample of the log by one of the lithotypes. Ideally the elastic parameter logs should be Backus averaged to the sample rate at which FFP will be applied on the available deterministic inversion results.
- Lithotypes can be differentiated by some combination of 1, 2 or 3 elastic parameters. The most common application of the method uses acoustic impedance and either shear impedance or  $V_p/V_s$ , but different combinations of elastic parameters can be examined using crossplots and/or histograms

to determine the set of elastic parameters which best discriminates between the different lithologies.

A crossplot of acoustic impedance versus  $V_p/V_s$  was colored by lithotypes and fitted with a probability density function (PDF). Normal Gaussian distribution of the log samples was used to create a joint PDF (Figure 7-1). The PDF incorporated statistical parameters, such as mean, standard deviation and correlation. These parameters were part of the model that described the statistical relationship between multiple properties derived from the seismic inversion process (acoustic impedance and  $V_p/V_s$ ). The summary of mean and standard deviation of elastic properties were defined to describe each PDF which were used in lithofacies classification (Table 7-1).

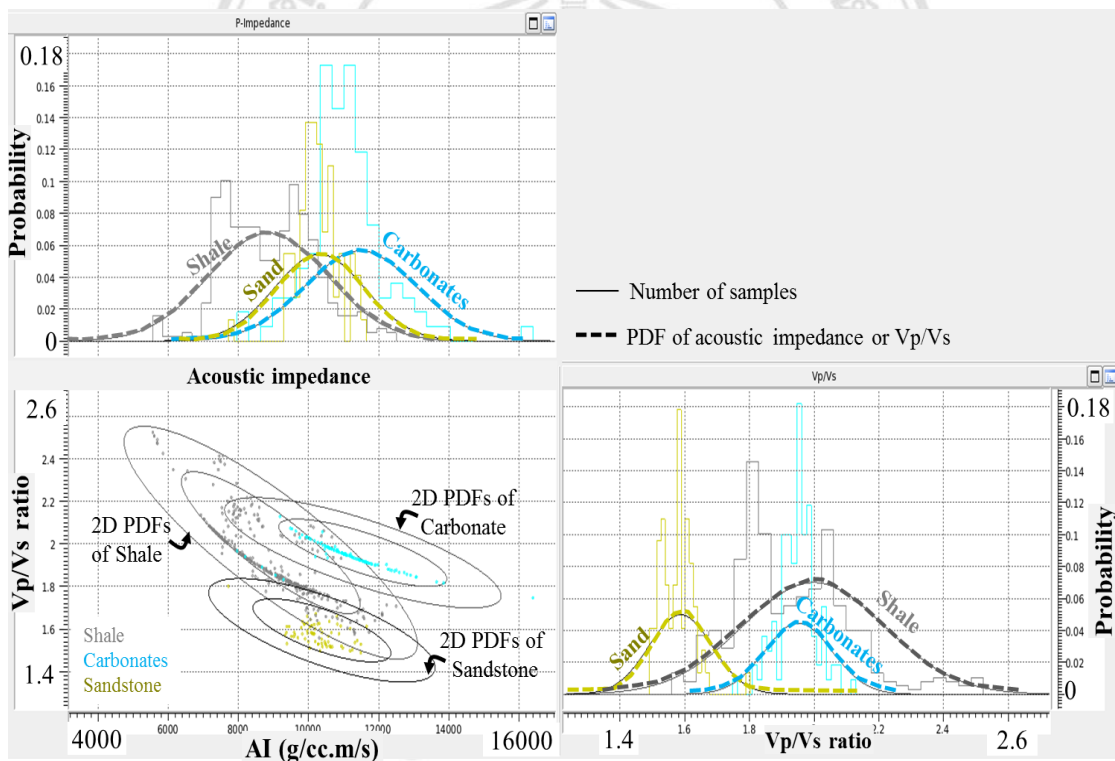


Figure 7-1 Probability density functions were derived using the crossplot of elastic properties (acoustic impedance versus  $V_p/V_s$ ) colored by lithotypes extracted from well log data for shale, carbonates and sandstone.

Table 7-1 Normal distributions were derived for each lithotype.

Lithology Types	AI (g/cc.m/s)		Vp/Vs	
	Mean	Standard deviation	Mean	Standard deviation
<b>Shale</b>	8851	1681	2.00	0.22
<b>Carbonates</b>	11475	1585	1.95	0.10
<b>Sandstone</b>	10310	1299	1.59	0.10

The prior probabilities of each lithotype were estimated using a lithology log that indicated the relative proportion of each expected lithology within the region of interest. A histogram of the available lithotype logs from the wells was made according to lithotypes and calculating the relative proportion of each lithotype found in the zone of interest (Figure 7-2). Shale had the highest prior probability at 0.615, followed by carbonate with a probability of 0.230, while sandstone had the lowest probability at 0.155. The lithotype-conditioned PDFs and a priori geological information were combined within a Bayesian inference framework to generate lithology probability volumes from the inverted elastic parameter volumes. Following Bayes' rule, the prior probability is used in the calculations of the posterior probabilities of each of the selected lithologies;

$$P(\text{litho log } y_i | \text{input}) = \frac{P(\text{input} | \text{litho log } y_i) * P(\text{litho log } y_i)}{\sum P(\text{input} | \text{litho log } y_i) * P(\text{litho log } y_i)}$$

where  $i$  is the index for a particular lithotype,  $input$  is the inversion results,  $P(\text{litho log } y_i)$  is the prior probability,  $P(\text{input} | \text{litho log } y_i)$  is the selected PDF,  $P(\text{litho log } y_i | \text{input})$  is the posterior probability. Before applying to the inverted elastic properties, the posterior PDFs were normalized;

$$\sum P(\text{litho log } y_i | \text{input}) = 1$$

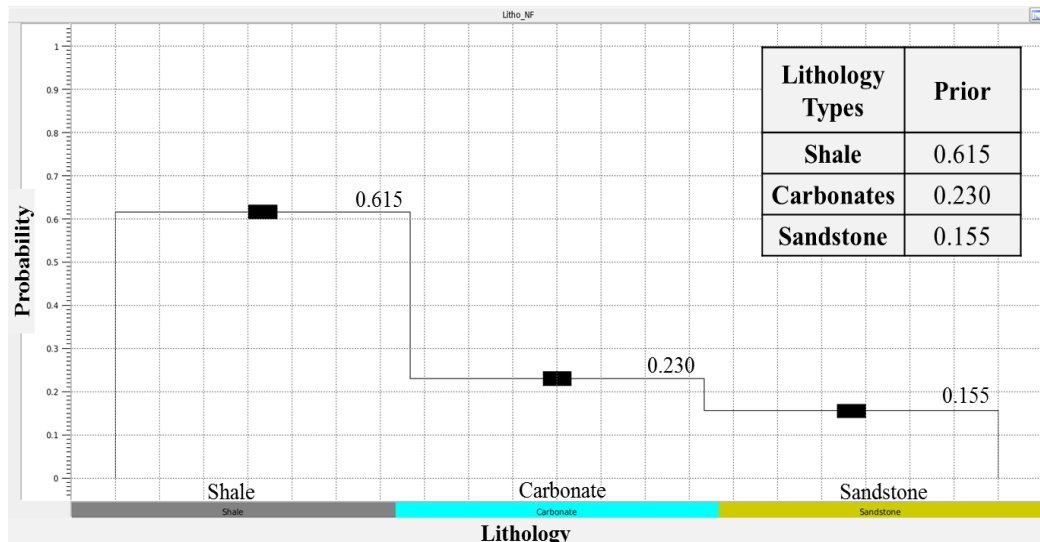


Figure 7-2 Prior probability for each lithology.

Figure 7-3 showed location of random line that passed through all wells. The final results of this process were lithofacies cube (highest probability), and probability cubes for each of the three lithology types considered in this study (shale, carbonate and sandstone), as shown in Figures 7-4 and 7-5. The lithofacie cube volume was calculated by comparing all lithology probability volumes per sample and retrieving the lithology that had the highest probability for that sample. (Additional results are available in APPENDIX D).

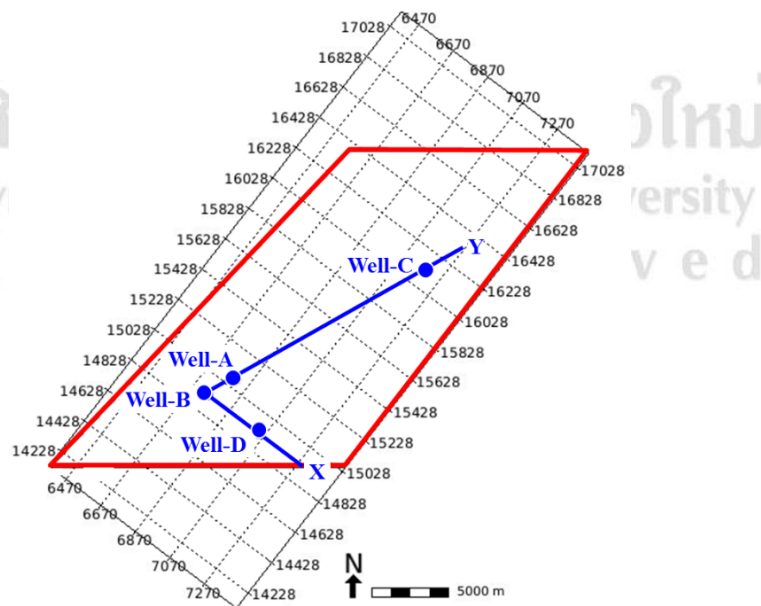


Figure 7-3 Location of random line which was used to show the final results.

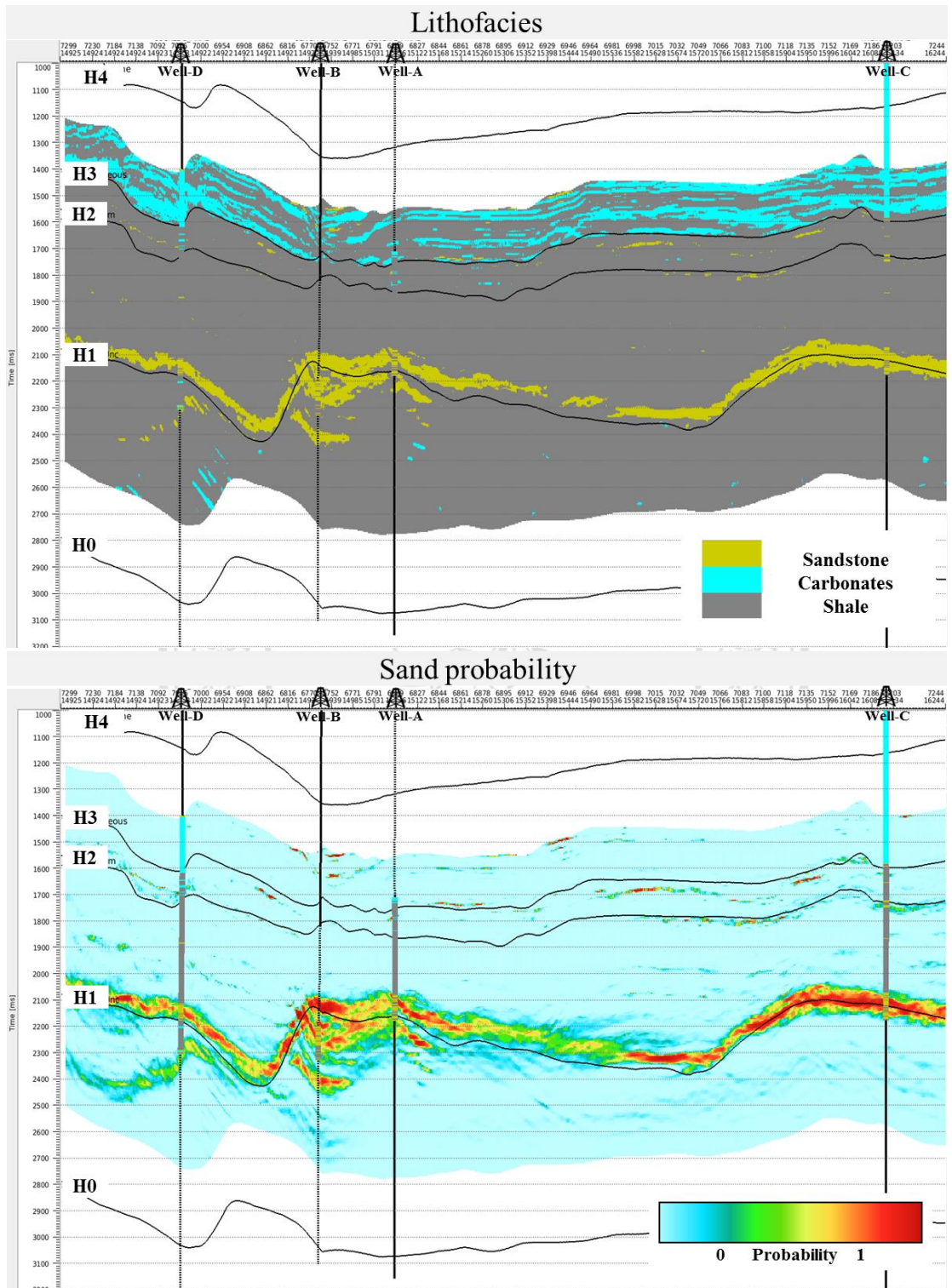


Figure 7-4 (Top) Random line showing the resulting lithofacies cube superposed with the lithology log at each well location colored by grey – shale, cyan – carbonate, yellow – sandstone. (Bottom) Random line showing the probability of sand superposed with the lithology log at each well location.

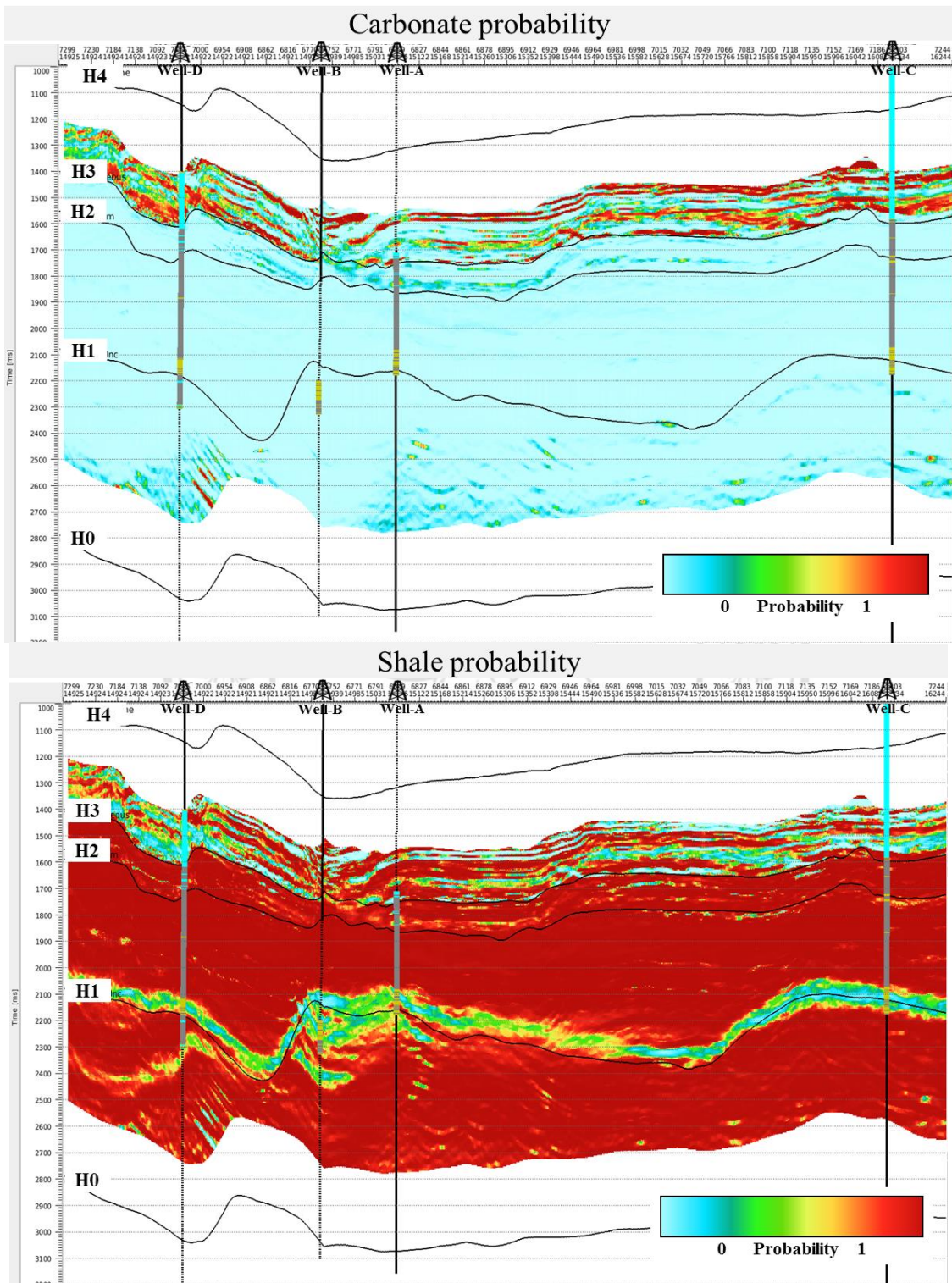


Figure 7-5 (Top) Random line showing the probability of carbonate, superposed with the lithology log at each input well location. (Bottom) Random line showing the probability of shale, superposed with the lithology log at each input well location.

A blind validation test was performed on Well-B to validate the final lithofacies estimation. Only limited measured Vp log was available at this well, which effected the elastic properties calculation (see Chapter 3). PDF's were derived using all well log data, also including Well-B, despite the limited portion of log data at this location (Figure 7-6 (left)). However, additional lithology logs at Well-B were prepared using a combination of gamma ray and other petrophysical interpreted logs (Figure 7-6 (right)). The results of the blind validation test at Well-B showed a good match between the lithology log and lithofacies extracted from inverted properties.

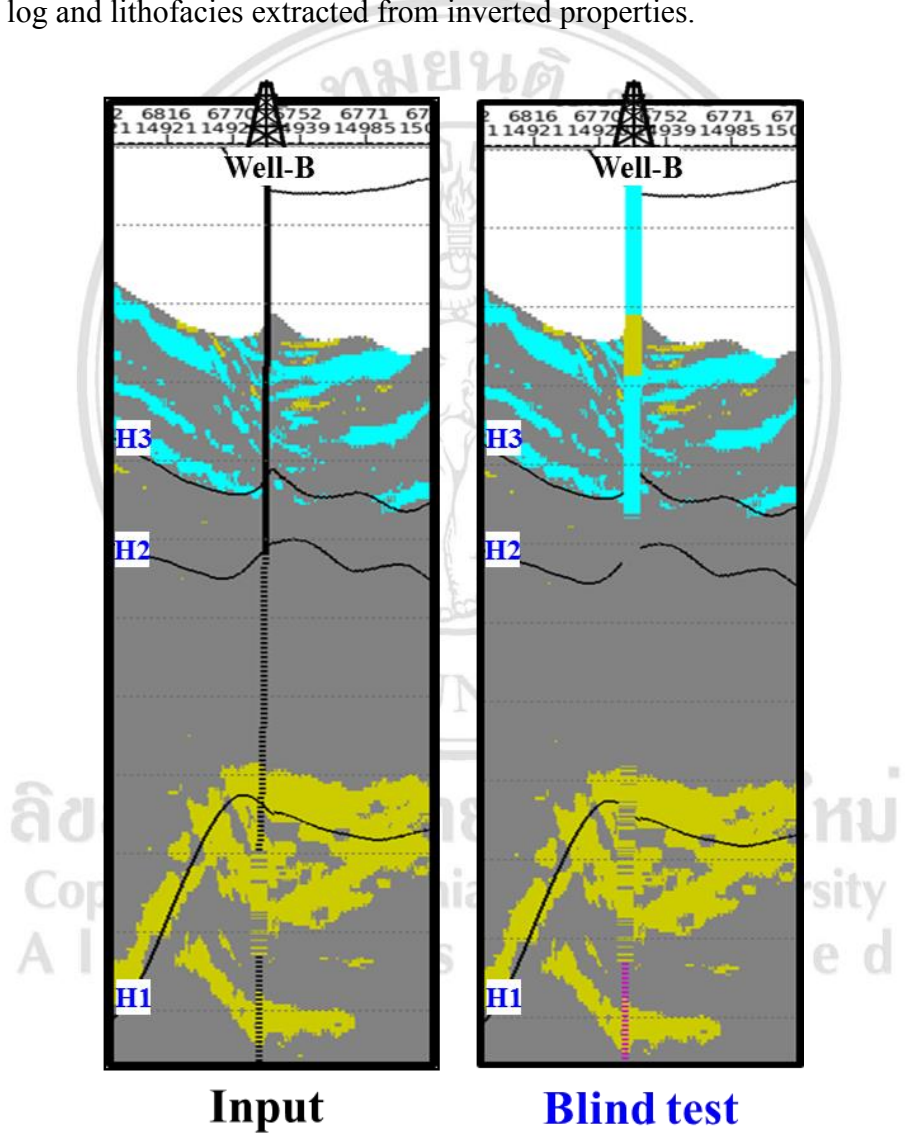


Figure 7-6 Comparison of lithofacies derived from inverted properties and Well-B lithology log. The original lithology log was only available within a short interval (left), so a more complete lithology log was estimated, using other available logs (right).

Seismic attribute maps were also produced, using the results from the seismic inversion and reservoir characterization study. Among the maps were produced lithology distribution and lithology probability along target horizons (Figure 7-7).

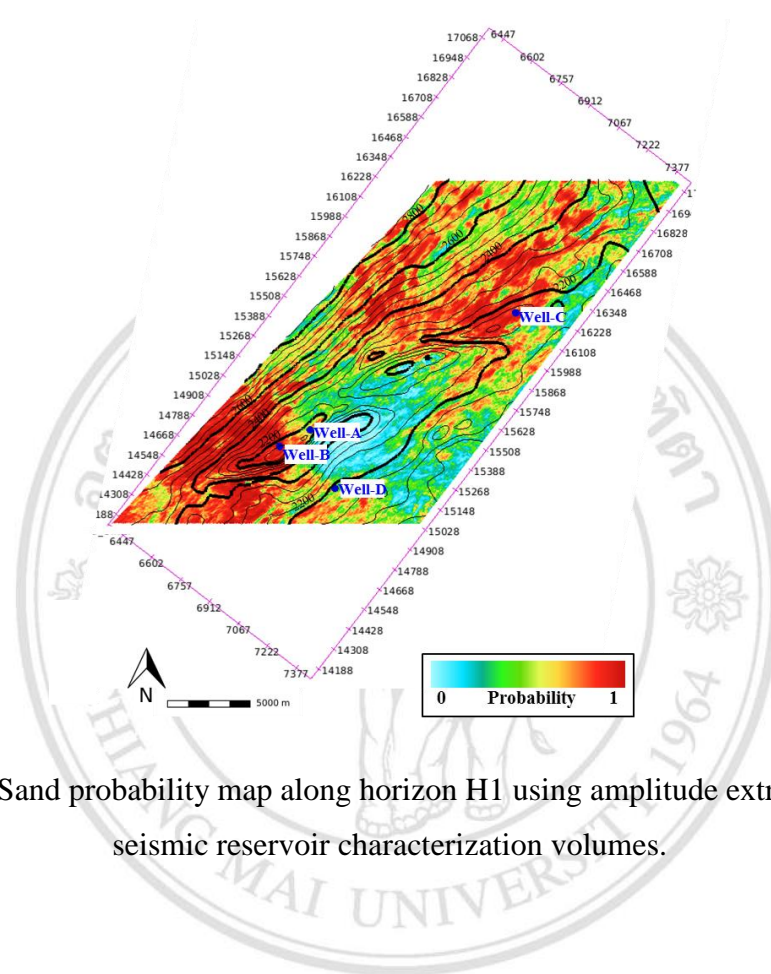


Figure 7-7 Sand probability map along horizon H1 using amplitude extraction from seismic reservoir characterization volumes.

ลิขสิทธิ์มหาวิทยาลัยเชียงใหม่  
Copyright© by Chiang Mai University  
All rights reserved